Modelling of a MEMS-based microgripper: application to dexterous micromanipulation

M. Boudaoud, Y. Haddab, and Y. Le Gorrec

***Abstract*—MEMS-based microgrippers with integrated force sensor have proved their efficiency to perform dexterous micromanipulation tasks through gripping forces sensing and control. For force control, knowledge based models are more relevant and gives better physical significance than the use of black box models. However this approach is often limited by many problems commonly encountered in the MEMS (micro electromechanical systems) structures such as: complex architectures, nonlinear behaviors and parameters uncertainties due to fabrication process at the micrometer scale. For these reasons theoretical approaches must be compared with experiments. This paper describes a modelling approach of a MEMS-based microgripper with integrated force sensor while handling micro-glass balls of 80µm diameter. Therefore, a state space representation is developed to couple both the dynamics of the actuation and sensing subsystems of the gripper through the stiffness of the manipulated object. A knowledge based model is obtained for small displacements at the tip of the gripper arms (small gripping forces) and is compared with experimental approaches. Good agreements are observed allowing interesting perspectives for the control.**

I. Introduction

Accurate and dexterous micromanipulation tasks are very important in a wide range of microrobotics applications such as microassembly tasks [1], minimally invasive surgery, genetics, in vitro fertilization, and cell mechanical characterization [2] [3] [4]. In this case, the use of microgrippers and controlling gripping forces applied on manipulated samples in the micrometer range (i.e. between *1µm* and *1mm*) without destroying and damaging is still a great scientific and technological challenge [5] [6]. This purpose requires reliable models which faithfully reflect the dynamic behavior of the microgrippers despite problems commonly encountered in microsystems such as complex architectures, nonlinear behaviors, and geometrical uncertainties. Moreover it is often difficult to conduct experiments in the microworld for models validations. In [7], it has been shown that suspensions used in the MEMS (micro electromechanical systems) structures such as clamped-clamped beams produces nonlinear behavior for large deflections, indeed their stiffness strongly increases with the deflection. Moreover variations in electrode dimensions and gap in electrostatic structures such as silicon comb drives cannot be neglected on the capacitance and coulomb forces [8]. Also, the mechanical properties of integrated suspensions are affected by their geometrical uncertainties [9].

M. Boudaoud, Y. Haddab, and Y. Le Gorrec are with the Automatic Control and Micro Mechatronic Systems Department, FEMTO-ST Institute, UFC-ENSMM-UTBM-CNRS, University of Franche-Comté, Besançon, France.
{ mokrane.boudaoud, yassine.haddab, legorrec }@femto-st.fr

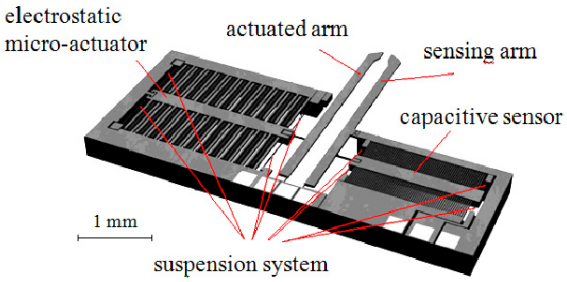

Fig. 1. Structure of the FT-G100 microgripper (FemtoTools GmbH).

To deal with these limitations, black box models viewed solely in terms of its input, output are often used to predict systems behavior with no a priori information about internal properties of controlled systems [10], although a knowledge of these parameters allows a better physical significance and offers the possibility to adapt MEMS models when changing physical design parameters. Knowledge based models are in this case more suitable for control, however, this approach requires comparing theoretical results with experiment because of previously cited problems.

The aim of this paper is the modelling of a silicon MEMS-based microgripper (Fig.1) when handling 80µm glass balls. The modelling approach is conducted taking into account internal parameters of the manipulation system. This microgripper (FT-G100 FemtoTools GmbH) uses an electrostatic actuator and an integrated force sensor allowing dexterous micromanipulation tasks. Some of its recent microrobotic applications can be found in [11] and [12]. In this study, at first, both actuated and sensing subsystems are modeled using theoretical approaches and no linear behaviors are discussed. After that, a coupled model of the gripper is then proposed in the state space representation when the gripper arms are closed around the manipulated object (80µm glass ball), thus the obtained model couple the dynamical behavior of the actuated and sensing subsystems thought the stiffness of the manipulated object. Unknown parameters of the gripper are identified using experimental data and least squares identification method (Levenberg–Marquardt algorithm). For weak gripping forces, it has been shown that the coupled model obeys to linear behavior.

Good agreements have been observed between analytical and experimental approaches of the coupled model, allowing interesting perspectives for the force control.

II. PRESENTATION AND WORKING PRINCIPLE OF THE FT-G100 MICROGRIPPER

A. Structure of the gripper

The FT-G100 microgripper is a silicon device that features two main parts: an electrostatic lateral comb-drive actuator which generates the displacements of an actuated arm, and a capacitive force sensor attached to a sensing arm with a resolution of *50nN*. This monolithic gripper is designed in order to handle objects ranging from *1µm* to *100µm*. The initial opening of the gripper is *100µm* and the full close is achieved while applying the maximum actuation voltage (*200V*).

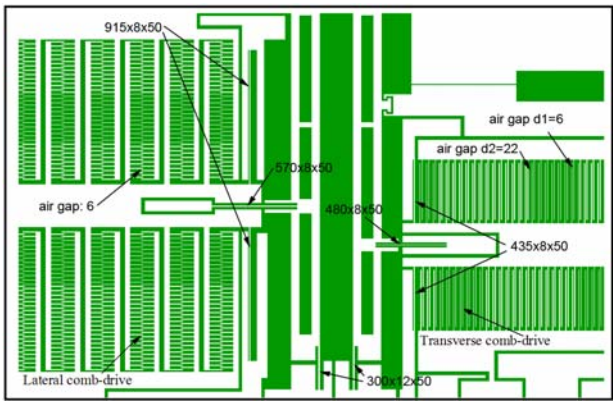

Fig. 2. Internal dimensions of the FT-G100 microgripper (FemtoTools GmbH).

B. Working principle

To pick up a micro-object, the actuated arm is pushed toward closure thanks to Coulomb forces generated by the electrostatic actuator. Furthermore a spring suspension system including two pairs of clamped-clamped beams holds the movable part of the actuator and produces a restoring force aimed to counteract the electrostatic action. While the gripper arms are closed around a micro-object, the deflection of the sensing arm is detected by the capacitive sensor. This last consists of a transverse comb-drive with a differential capacity ΔC proportional to the displacement x_{eb} of the movables electrodes. This displacement is due to the applied force on the tip of the sensing arm (i.e. the gripping force) and is translated into analog voltage V_{out} throughout a MS3110 readout chip (Irvine Sensors Corp, Costa Mesa, Ca, USA). Two pairs of clamped-clamped beams are also attached to the moving part of the sensor and the restoring force F_{sb} is given by:

$$F_{sb} = K_{sb}.x_{eb} \quad (1)$$

K_{sb} is the total stiffness of the two pairs of clamped-clamped beams within the sensor. This parameter is considered invariant for small values of x_{eb}. For more details about the comb-drives used as actuators and sensors, refer to [13] [14].

III. MODELLING AND IDENTIFICATION

As the gripping force appears when the gripper arms are in contact with the manipulated object, a coupled model of the gripper has been used in order to take into account both dynamics of the actuated subsystem (actuator + actuated arm) and the sensing one (sensing arm + capacitive sensor) (Fig.3). The actuated and sensing subsystems are first modelled when an external force is applied at the tip of the gripper arms. Thereafter a simple modelling of the manipulated object is used to couple previous subsystems in the state space representation. Internal dimensions of the FT-G100 microgripper provided by femtotools technical support "support@femtotools.com" are used for the modelling approach. Higher dynamics of each subsystem are neglected considering that their effects are not significant in this study. Only second order models are then considered.

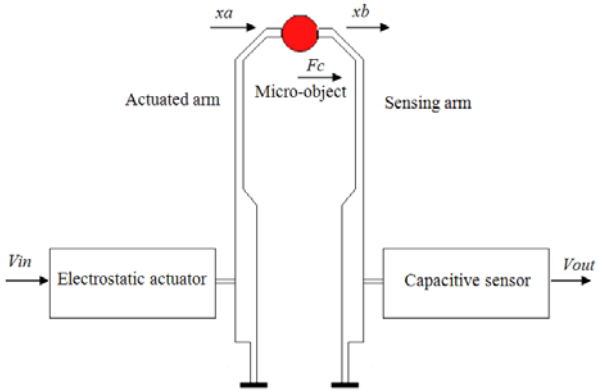

Fig. 3. System modelling.

A. Dynamic modelling of the actuated system

In open loop, the dynamical behavior of the actuated subsystem is observed while applying step voltages to the lateral comb drive actuator. The resulting displacements x_a at the tip of the actuated arm are recorded using a laser interferometer (SP-120 SIOS Meßtechnik GmbH). In fig.4 an example of normalised step responses of the considered system are presented for actuation voltages of *70 Volts*, *100 Volts*, *120 Volts* and *150 Volts*. It can be seen that the dynamical behavior changes with the applied actuation voltage. Moreover, the resonance frequency of this system increases with increasing the actuation voltage (Fig.5).

Considering that the mass of the system is invariant in all the operating range of the actuated subsystem, the increase of the resonance frequency is mainly due to the suspension's stiffness which increases for large deflections of the two pairs of clamped-clamped beams; this interpretation is in accordance with [7]. To get an accurate knowledge based model of the actuated subsystem in a wide working range, it is important to model the nonlinearities of the suspensions stiffness. Such kind of models can be found in [8]. However,

in this study only small deflections are considered, in fact the range of gripping forces applied by the gripper does not require large displacement of the actuated arm around a considered operating point. In this case non linear models are not considered, and the focus is only given to the dynamical behavior of the gripper while applying small gripping forces. This allows describing the corresponding dynamical behavior with linear models.

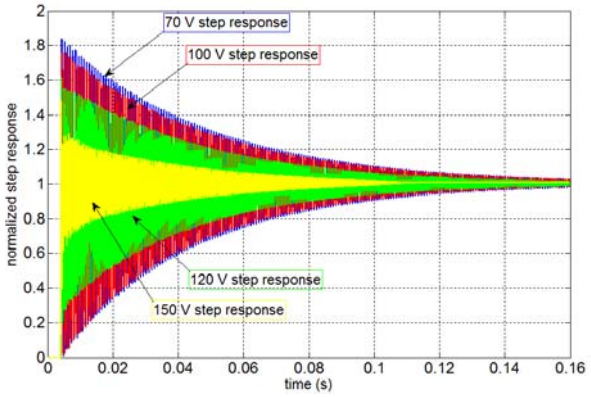

Fig. 4. Step responses of the actuated subsystem.

Besides, since the size of the grasped objects is about *80 µm*, a work around V_{in0} *=70V* is chosen. This actuation voltage allows a displacement of *20µm* in static mode at the tip of the actuated arm. Moreover a consideration is giving to the dynamical behavior of the actuated system while an external mechanical force F_c (i.e griping force) is applied at the tip of the actuated arm. Note that due to F_c, the resonance frequency of the actuated subsystem will significantly decrease.

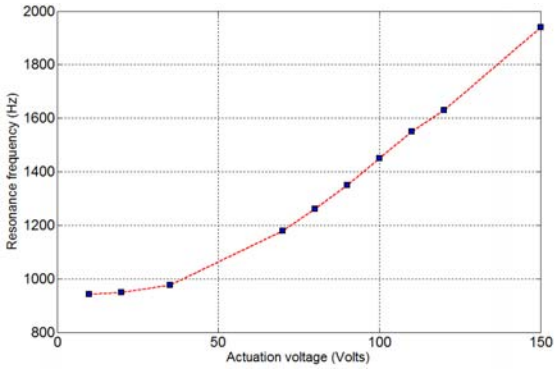

Fig. 5. Resonance frequencies of the actuated subsystem.

Using the fundamental law of dynamics, and considering as external forces: the electrostatic force F_x, and the gripping force F_c:

$$\sum \vec{F} = M_a \frac{\partial^2 x_{ea}}{\partial t^2} \Rightarrow F_x - K_{fa} \frac{\partial x_{ea}}{\partial t} - K_{sa}.x_{ea} - D_a.F_c = M_a \frac{\partial^2 x_{ea}}{\partial t^2} \quad (2)$$

K_{sa} is the total stiffness of the two pairs of clamped-clamped beams of the actuator, x_{ea} is the displacement of the movable electrodes of the actuator, D_a is an amplification parameter, and K_{fa} and M_a are respectively the damping factor, and the total mass of the actuated system.

Considering a hinge joint located at a distance *l/2* from the actuated arm clamp (Fig.6). The amplification parameter is given by:

$$D_a = \frac{x_a}{x_{ea}} = \frac{H - l/2}{a + l/2} \quad (3)$$

Where: *H=5300µm*, *l=300µm* and *a=950µm*, are some specific dimensions of the actuated arm (Fig.6).

Otherwise, by applying the Bernoulli's principle on the two pairs of clamped-clamped beams with a punctual load applied in the middle, the stiffness K_{sa} can be expressed as follow:

$$K_{sa} = 32 \frac{E.h.w^3}{L_1^3} \quad (4)$$

Where *E= 190GPA* is the Young's modulus of the silicon beams, and L_1*=1830µm*, *w=8µm* and *h=50µm* are their length, width, and thickness respectively (Fig.2).

Moreover, the analytical expression of the electrostatic force generated by the lateral comb-drive actuator is given by [13]:

$$F_x = \frac{N_a.\varepsilon.h}{2.g.} V_{in}^2 \quad (5)$$

Where ε *=8.85pF/m* is the permittivity of the dielectric material (air) between the comb's fingers, N_a*=1300* is the number of the pairs of electrodes in the actuator, and *g=6µm* is the gap between two fingers.

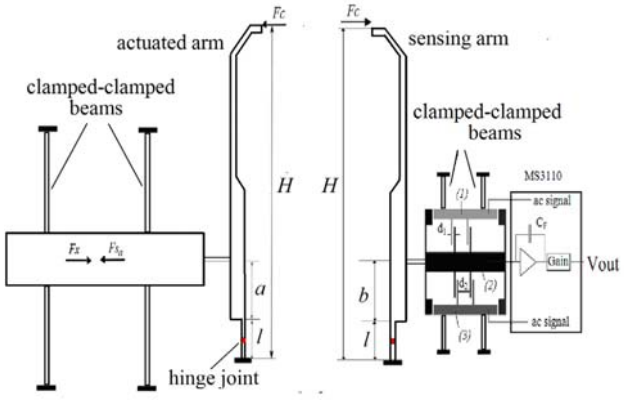

Fig. 6. Actuated and sensing subsystems.

A sufficient approach for modelling the manipulated micro-object is to consider its effective mass m_{eff}, its viscous damper v_d and its stiffness k_0 [15]. Such kind of models needs accurate study on micro-objects behaviors. However, in a first approach it is possible to assume that the grasped micro-object behaves as a spring with a stiffness k_0 [16]. In this case, the analytical expression of the gripping force is then given by:

$$F_c = k_0.(x_a - x_b) = k_2.x_b \Rightarrow x_b = \frac{k_0}{k_0 + k_2} x_a \quad (6)$$

Then:

$$F_c = \frac{k_0.k_2}{k_0 + k_2} x_a = k_k.x_a \quad (7)$$

k_2 is the sensing system's stiffness, and x_b is the deflections at the tips of the sensing arm.

Moreover, near a desired operating point (V_{in}=V_{in0}, x_a=x_{a0}), a linear relation can be expressed between small variations of both the supply voltage $\tilde{V}_{in}$ and the actuated arm tip displacement $\tilde{x}_a$:

$$\frac{M_a}{D_a}.\frac{\partial^2 \tilde{x}_a}{\partial t^2}+\frac{K_{fa}}{D_a}.\frac{\partial \tilde{x}_a}{\partial t}+\left(\frac{K_{sa}}{D_a}+D_a.k_k\right).\tilde{x}_a=\frac{N_a.\varepsilon.t.V_{in0}}{g}\tilde{V}_{in} \quad (8)$$

Finally an analytical second order model can be obtained allowing the description of the dynamic behavior of the actuated system near the desired operating point. Its expression is given by:

$$G_a(s)=\frac{\tilde{X}_a(s)}{\tilde{V}_{in}(s)}=\frac{D_a}{g}\frac{N_a.\varepsilon.t.V_{in0}}{M_a.s^2+K_{fa}.s+(K_{sa}+D_a^2.k_k)} \quad (9)$$

s is the Laplace variable.

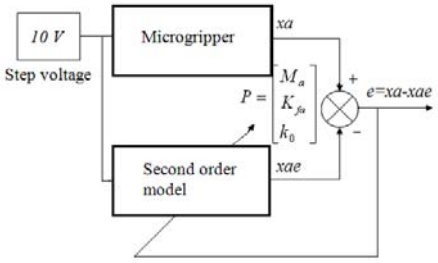

(a)

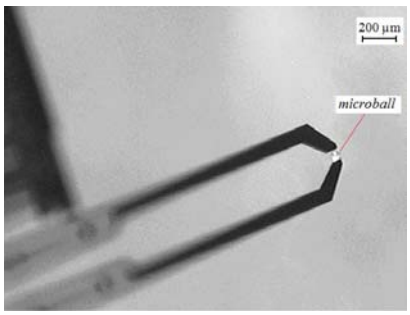

(b)

Fig. 7. (a) Parameter identification, (b) photography of the FT-G100 handling the 80µm glass-ball.

The numerical values of known parameters are provided by the FemtoTools technical support, which lead to: D_a=*4.7* and K_{sa}=*25.4N/m*. The other parameters such as the damping factor and the total mass of the actuated system will be obtained by identification.

B. *Actuated system identification*

The parameters M_a , K_{fa} , and k_0 are estimated using a least square identification method (Levenberg–Marquardt algorithm). Therefore the electrostatic actuator has been excited with a *10V* step voltage around the operating point while the object seizure was happening. The record of the step response x_a was performed with a low measurement noise thanks to the laser interferometer. The identification algorithm leads to obtaining the parameter vector $\boldsymbol{p}$=*[* M_a K_{fa} k_0*]*^{T} which minimize a quadratic criterion of the error e between the measured displacement x_a and the estimated one x_{ae}. The estimation algorithm lets obtain: M_a =*1.37mg*, K_{fa} =*1.3mNs²/m*, and k_0 =*1043 N/m*. Note that these values may slightly differ due to over- or under etching of the MEMS device.

Translating the transfer function $G_a(s)$ (Equa.9) into discrete state space representation using matlab software with a *20Khz* sampling frequency, a controllable form can be expressed as:

$$\begin{cases}\boldsymbol{x}_1(k+1)=\boldsymbol{A}_a.\boldsymbol{x}_1(k)+\boldsymbol{B}_a.V_{in}(k)\\ x_a(k)=\boldsymbol{C}_a.\boldsymbol{x}_1(k).\end{cases} \quad (10)$$

$$\boldsymbol{A}_a=\begin{pmatrix}1.6621 & -0.9536\\ 1 & 0\end{pmatrix}\quad \boldsymbol{B}_a=\begin{pmatrix}0.25\\ 0\end{pmatrix}$$
$$\boldsymbol{C}_a=\begin{pmatrix}0.1104 & 0.1086\end{pmatrix}$$

$\boldsymbol{x}_1\in\Re^{2\times1}$, $\boldsymbol{A}_a\in\Re^{2\times2}$, $\boldsymbol{B}_a\in\Re^{2\times1}$ and $\boldsymbol{C}_a\in\Re^{1\times2}$ are the state vector, state matrix, input matrix, and output matrix, respectively of the actuated subsystem.

C. *Dynamic modelling of the sensing system*

When the gripping force F_c is applied at the tip of the sensing arm, the dynamic behavior of the sensing subsystem can be expressed as follow:

$$\sum\vec{F}=M_b\frac{\partial^2 x_{eb}}{\partial t^2}\Rightarrow D_b.F_c-K_{fb}\frac{\partial x_{eb}}{\partial t}-K_{sb}.x_{eb}=M_b\frac{\partial^2 x_{eb}}{\partial t^2} \quad (11)$$

D_b is an amplification parameter, and K_{fb} and M_b are respectively the damping factor, and the total mass of the sensing subsystem.

As for the actuated subsystem assumptions:

$$D_b=\frac{x_b}{x_{eb}}=\frac{H-l/2}{b+l/2} \quad (12)$$

Also:

$$K_{sb}=32\frac{E.h.w^3}{L_2^3} \quad (13)$$

L_2 is the length of the clamped-clamped beams of the sensor. The dynamic behavior expression (Equa.11) becomes:

$$M_b.\frac{\partial^2 x_b}{\partial t^2}+K_{fb}.\frac{\partial x_b}{\partial t}+K_{sb}.x_b=D_b^2.F_c \quad (14)$$

This leads to the transfer function:

$$G_b(s)=\frac{X_b(s)}{F_c(s)}=\frac{D_b^2}{M_b.s^2+K_{fb}.s+K_{sb}} \quad (15)$$

In addition with previous given numerical values of known parameters: b=*700µm* , L_2=*870µm*

Then: D_b=*6.05* and *Ksb=235.36N/m*

Besides the stiffness can now be numerically evaluated with the analytical approach, as:

$$k_2 = \frac{K_{sb}}{D_b^2} \tag{16}$$

Then: k_2=6.45N/m

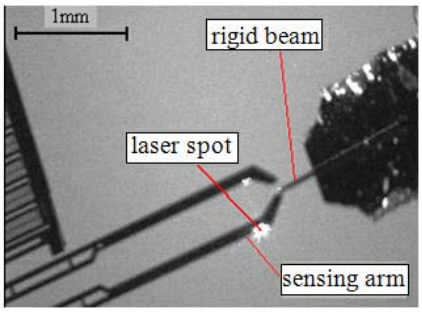

Fig. 8. Sensing arm excitation.

D. Sensing system identification

A step force is needed for the identification of the sensing subsystem. However it is not easy to generate such kind of signal. A negative step force has been then used by pushing up the tip of the sensing arm with a rigid beam (Fig.8) until a desired position and operating thereafter a fast withdrawal of the beam. The resulting motion of the arm tip is recorded using the laser interferometer previously cited.

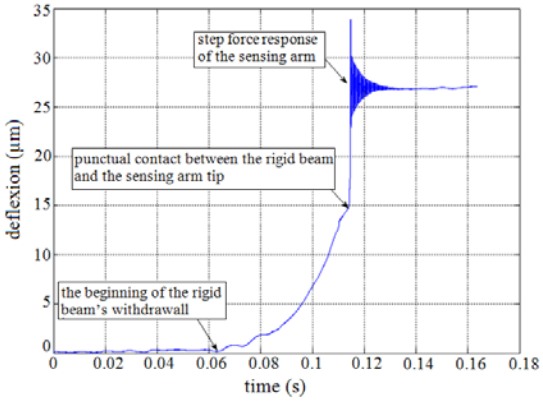

Fig. 9. Position response of the sensing arm tip to a 27µm thrust.

In Fig.9, is shown an example of a position response for a *27µm* thrust. Note that this position response will be further translated into force information by taking into account the stiffness of the sensing system. Moreover, in order to deduce the real input force from the applied sensing arm thrust, the static 'force/arm tip displacements' characteristic of the sensing system has been plotted aimed to determine experimentally its stiffness. Therefore the sensor's output voltage has been used to evaluate each force corresponding to known displacements of the arm tip. As shown in Fig.10 the force sensor obeys to a linear behavior and is able to detect forces up to *140µN*. The stiffness k_2 of this system is evaluated at about *6.48N/m*. The analytical approach led us to obtain k_2 =6.45N/m. The difference is due to uncertainties in the given numerical values of the system dimensions caused by the microgripper fabrication process. Nevertheless in this study, the obtained values of k_2 are not so far one from the other.

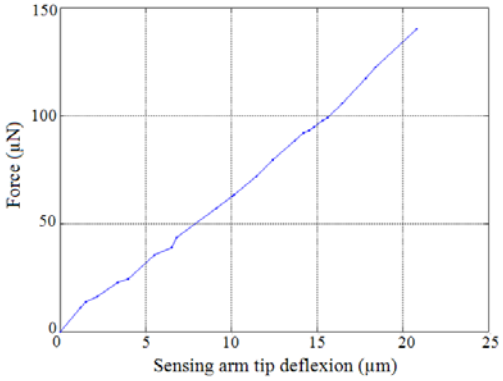

Fig. 10. Static force/position characteristic of the sensor.

Using the previous identification method, and exploiting the obtained step response of the sensing subsystem, the unknown parameters of this last have been estimated, and the obtained results are: M_b =0.5mg and K_{fb} =0.71mNs²/m.

For a *20Khz* sampling frequency the corresponding discrete state space representation of (Equa.15) is given as:

$$\begin{cases} \boldsymbol{x}_2(k+1) = \boldsymbol{A}_c.\boldsymbol{x}_2(k) + \boldsymbol{B}_c.F_c(k) \\ x_b(k) = \boldsymbol{C}_c.\boldsymbol{x}_2(k). \end{cases} \tag{17}$$

$$\boldsymbol{A}_c = \begin{pmatrix} 1.142174 & -0.947527 \\ 1 & 0 \end{pmatrix} \quad \boldsymbol{B}_c = \begin{pmatrix} 0.5 \\ 0 \end{pmatrix}$$
$$\boldsymbol{C}_c = \begin{pmatrix} 0.132080 & 0.129656 \end{pmatrix}$$

$\boldsymbol{x}_2 \in \Re^2, \boldsymbol{A}_c \in \Re^{2\times2}$, $\boldsymbol{B}_c \in \Re^{2\times1}$ and $\boldsymbol{C}_c \in \Re^{1\times2}$ are the state vector, state matrix, input matrix, and output matrix, respectively of the sensing system.

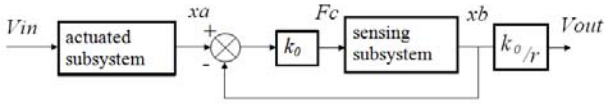

Fig.11. Bloc diagram of the coupled model of the gripper.

E. Gripper Modelling

For the gripper modelling actuated and sensing subsystems' states are coupled under the assumption that the grasped micro-object behaves as a spring with a known stiffness k_0. Using the analytical expression of the griping force (Equa.7), previous subsystem's state space models can be unified to obtain the following state space representation according to the whole micro-manipulation system:

$$\begin{cases} \begin{bmatrix} \boldsymbol{x}_1(k+1) \\ \boldsymbol{x}_2(k+1) \end{bmatrix} = \begin{bmatrix} \boldsymbol{A}_a & 0 \\ \boldsymbol{B}_c.k_k.\boldsymbol{C}_a & A_c \end{bmatrix} \cdot \begin{bmatrix} \boldsymbol{x}_1(k) \\ \boldsymbol{x}_2(k) \end{bmatrix} + \begin{bmatrix} \boldsymbol{B}_a \\ 0 \end{bmatrix} V_{in}(k) \\ Vout(k) = \begin{bmatrix} 0 & k_2/r.\boldsymbol{C}_c \end{bmatrix} \cdot \begin{bmatrix} \boldsymbol{x}_1(k) \\ \boldsymbol{x}_2(k) \end{bmatrix} \end{cases} \tag{18}$$

r is the sensor's sensitivity. (*50 N/Volts*)

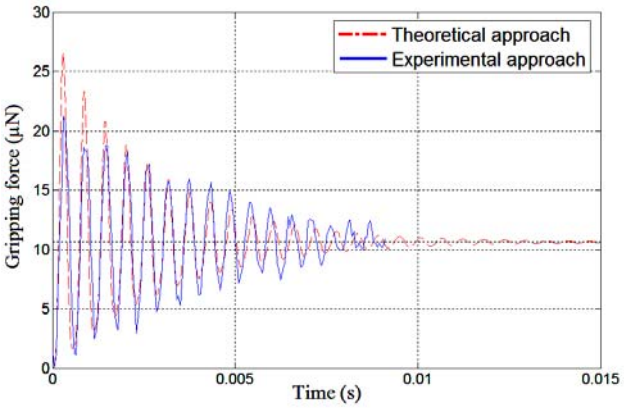

Fig.12. Step responses of the coupled micro-manipulation system according to a 10 *V* actuation voltage.

IV. DISCUSSION

When handling the 80 µm glass ball, both *10V* (around V_{in0} *=70V*) step responses of the knowledge based model and the one recorded experimentally from the output of the force sensor are presented in Fig. 12. The dynamics of the real manipulation system and that of the model are close to each other. The pseudo natural frequency of the model is near to the real one, this corresponds to a good estimation of the system stiffness and mass. Besides in static mode the two step responses are in accordance and reach *11µN*. However, taking into account damping phenomena at micro scale such as the interaction of the movable structure of the gripper with the surrounding fluid of a certain viscosity is needed to an accurate estimation of the damping factor, which is not a simple approach. More accurate estimation of the gripper internal parameters requires expensive equipment and tedious experiments while simple approaches can provide reliable models for control. Nevertheless the obtained coupled model of the gripper reflects an important part of the real system dynamics. Lack of dynamics information can be even compensated with appropriate controllers

V. CONCLUSION

A modelling approach of a MEMS-based microgripper is presented while handling a micro-glass ball of 80 µm diameter. The developed knowledge based model couples the dynamics of the actuation and the sensing subsystems of the microgripper through the manipulated object stiffness. It is even possible to adjust the coupled model when changing physical design parameters of the microgripper, also different kind of micro-objects can be considered with this model in the limit of the given assumptions. Good agreements are observed between theoretical and experimental approaches allowing interesting perspectives for dexterous micromanipulation tasks through force controllers. Future work will concern modelling of the actuated subsystem in a wide working range taking into account nonlinearities of its suspensions. Moreover a hybrid force/position controller will be investigated to control the motion of the actuated arm position before contact with the manipulated object and to impose a controlled gripping force dynamic when the gripper arms are full closed around the considered manipulated object.

REFERENCES

[1] C. Clévy, A. Hubert and N. Chaillet, "Flexible micro-assembly system equiped with an automated tool changer", *Journal of Micro-Nano Mechatronics*, Vol .4, No.1-2, pp.59-72, 2008.

[2] A. Menciassi, A. Eisinberg, G. Scalari, C. Anticoli, M.C. Carrozza and P. Dario, "Force feedback-based microinstrument for measuring tissue properties and pulse in microsurgery", *in Proceedings of the IEEE International Conference on Robotics & Automation*, Vol. 1, pp.626-631, 2001.

[3] Y. Sun, K.T. Wan, K.P. Roberts, J.C. Bischof and B.J. Nelson, "Mechanical property characterization of mouse zona pellucida", *in IEEE Trans Nanobioscience.*,Vol 2, pp 279-286, 2003.

[4] X.Y. Liu, K.Y. Kim, Y. Zhang, and Y. Sun, "Nanonewton force sensing and control in microrobotic cell manipulation", *in international Journal of Robotics Research*, Vol. 28, No. 8, pp. 1065-1076, 2009.

[5] K. Kim, X. Liu, Y. Zhang, and Y. Sun, "Micronewton force-controlled manipulation of biomaterials using a monolithic MEMS microgripper with two-axis force feedback", *in IEEE International Conference on Robotics and Automation*, pp. 3100-3105, 2008.

[6] A. Eisinberg, A. Menciassi, S. Micera, D. Campolo, M. C. Carrozza, and P. Dario, "PI force control of a microgripper for assembling biomedical microdevices", *in IEEE proceedings, Circuits, devices and systems*, Vol. 148, N. 6, pp. 348-352, 2001.

[7] R. Legtenberg, A. Groeneveld, and M. Elwenspoek, "Combdrive actuators for large displacements", *Journal of Micromechanics and Microengineering*, Vol. 6, pp. 320–329, 1996.

[8] Frisch-Fay R 1962 *Flexible bars* (London: Butterworths).

[9] N. Agarwal and N. R. Aluru, "A stochastic Lagrangian approach for geometrical uncertainties in electrostatics", *J. Comput. Phys*, Vol.226, Issue 1, pp. 156–179, 2007.

[10] Y.Haddab and B.Uccheddu, "Commande robuste d'une pince microfabriquée à actionnement électrostatique*", in Conférence Internationale Francophone d'Automatique*, 2008.

[11] F. Beyeler, S. Muntwyler, Z. Nagy, C. Graetzel, M. Moser, and B. J. Nelson, "Design and calibration of a MEMS sensor for measuring force and torque acting on a magnetic microrobot", *in Journal of Micromechanics and Microengineering*, Vol.18, p. 025004, 2008.

[12] A. Neild, S. Oberti, F.Beyeler, J. Dual and B. J. Nelson, "A micro-particle positioning technique combining an ultrasonic manipulator and a microgripper", *in Journal of Micromechanics Microengineering,* Vol. 16, pp. 1562-1570, 2006.

[13] W. A. Moussa, H. Ahmed, W. Badawy, and M. Moussa, "Investigating the reliability of electrostatic comb-drive actuators used in microfluidic and space systems using finite element analysis", *in Can. J. Elect. Comput. eng*, Vol. 27, No. 4, pp. 195–200, 2002.

[14] Y. Sun, and B.J. Nelson, "MEMS capacitive force sensors for cellular and flight biomechanics", *in Biomedical Materials*, Vol. 2, No. 1, pp. 16-22, 2007

[15] S. D. Eppinger and W. P. Seering, "On dynamic models of robot force control", *in Proceedings of the IEEE International Conference on Robotics & Automation*, pp. 29-34, 1986.

[16] M. Rakotondrabe, Y. Haddab and P. Lutz, "Modelling and control of a highly modular microassembly system", *in International Workshop on MicroFactory*, pp. 140-145, 2004.